Scientia Iranica B (2013) 20 (2), 322–328

Sharif University of Technology

Scientia Iranica

Transactions B: Mechanical Engineering

www.sciencedirect.com

Collocated Discrete Least Squares (CDLS) meshless method for the simulation of power-law fluid flows

M. Lashckarbolok *, **E. Jabbari**

School of Civil Engineering, Iran University of Science and Technology, Iran

Received 9 January 2012; revised 19 October 2012; accepted 8 January 2013

KEYWORDS

Meshless method;
Generalized Newtonian fluid;
Least squares technique;
Power-law fluids.

Abstract Least squares is a robust and simple method in function approximation. Collocated Discrete Least Squares (CDLS) is a meshless method based on least squares technique. In this paper CDLS is used with a non-incremental projection method for the solution of incompressible generalized Newtonian fluid flow equations in the simulation of laminar flow of power-law fluids. The scheme is used to solve two benchmark problems named lid-driven cavity flow and flow past a circular cylinder for the power-law fluids.

1. Introduction

Using a mesh or grid is a basic characteristic of the conventional numerical methods for the solution of the partial differential equations. During the recent years, considerable effort has been devoted to developing the so-called meshless methods. The purpose of the methodology is to get rid of at least the structure of the mesh and to approximate the solution using scattered nodes inside and on the boundaries of the domain. A detailed review on the meshless methods has been provided by Belytschko [1], Liu [2] and Liu and Gu [3]. Each efficient numerical method should possess some properties such as strong mathematical basis, simplicity and efficiency. The mathematical basis of CDLS is the least squares technique. Since the method enjoys symmetric and sparse matrices it is efficient in computational cost. The main idea was adopted from least squares technique in FEM. Afshar and Arzani developed Discrete Least Squares (DLS) meshless method for the solution of convection-dominated problems [4]. Afshar and Lashckarbolok used collocation points in DLS method and developed CDLS meshless method [5]. They also presented a posteriori error estimate and an adaptive refinement strategy in conjunction with the method. According to their research, collocation points have significant effects on the performance of the method. Recent research on CDLS method has focused on the solution of incompressible Navier–Stokes equations. In this field Firoozjaee and Afshar used CDLS method for the solution of incompressible Navier–Stokes equations in its primitive form [6]. They proposed a semi-incremental fractional step method for the temporal discretization of the incompressible Navier–Stokes equations which can be applied to the solution of these equations using large time steps without any restrictions on satisfying the Ladyzhenskaya–Babuska–Brezzi (LBB) condition.

In the present study, the CDLS method is extended for the solution of incompressible generalized Newtonian fluid equations in the simulation of laminar flow of power-law fluids. The Radial Point Interpolation Method (RPIM) is used to construct shape functions. The proposed scheme is used to solve lid-driven cavity flow and flow past a circular cylinder for power-law fluids.

2. CDLS meshless method

Consider the following differential equation:

$$L(u) = f \quad \text{in } \Omega \tag{1}$$

$$B(u) = g \quad \text{on } \Gamma_t \tag{2}$$

$$u = \bar{u} \quad \text{on } \Gamma_u. \tag{3}$$

Here, u denotes the unknown function. L and B are some proper differential operators defined on the problem domain Ω and its

* Corresponding author. Tel.: +98 1715532070.
E-mail addresses: mlbolok@iust.ac.ir (M. Lashckarbolok), jabbari@iust.ac.ir (E. Jabbari).

Peer review under responsibility of Sharif University of Technology.

Production and hosting by Elsevier

1026-3098 © 2013 Sharif University of Technology. Production and hosting by Elsevier B.V. Open access under CC BY license.
doi:10.1016/j.scient.2013.02.010

Neumann boundary Γ_t, respectively. Γ_u represents the Dirichlet boundary with a prescribed value of $\bar{u}$ and f is the source term in the problem domain. The philosophy behind the least squares method is to find an approximate solution that minimizes the least squares functional to be defined later. As shown in Figure 1, the problem domain and its boundaries are discretized by nodal and collocation points. Assume that n_p is the number of nodes in the domain and on the boundaries. Beside the nodal points, the collocation points are used in the problem domain and on its boundaries. In this methodology in each nodal point one collocation point has to be placed as shown in Figure 1. Assume that M is the number of collocation points.

The approximated value of the function u at collocation point k with coordinate x_k, can be obtained through the following interpolation:

$$u(x_k) = \sum_{i=1}^{\bar{n}} N_i(x_k) \cdot u_i, \tag{4}$$

where u_i is the value of the unknown function at the ith nodal point. $\bar{n}$ is the number of nodal points that the kth collocation point with coordinate x_k, has in its domain. This idea of compact support is shown in Figure 2. To set up such a domain for each collocation point a radius ds is defined so that a specific number of nodal points are placed into its support domain. In Eq. (4), $N_i(x_k)$ is the value of the shape function of the ith node at the kth collocation point. In this paper first the number of nodes to support collocation points is defined as $\bar{n}$. Then for each collocation a radius (ds) is determined so that $\bar{n}$ nodes are placed in the domain of that collocation. Substitution of Eq. (4) into Eqs. (1)–(3) leads to the differential equation residual (R^d), the Neumann boundary condition residual (R^t) and the Dirichlet boundary condition residual (R^u) defined as follows respectively:

$$\begin{aligned} R_k^{(d)} &= L(u(x_k)) - f(x_k) \\ &= \sum_{i=1}^{\bar{n}} L(N_i(x_k))u_i + f(x_k) \quad (k = 1 \sim M) \end{aligned} \tag{5}$$

$$\begin{aligned} R_k^{(t)} &= B(u(x_k)) - g(x_k) \\ &= \sum_{i=1}^{\bar{n}} B(N_i(x_k))u_i - g(x_k) \quad (k = 1 \sim n_t) \end{aligned} \tag{6}$$

$$\begin{aligned} R_k^{(u)} &= u(x_k) - \bar{u} \\ &= \sum_{i=1}^{\bar{n}} (N_i(x_k))u_i - \bar{u} \quad (k = 1 \sim n_u). \end{aligned} \tag{7}$$

In these relations, n_t and n_u are the number of collocation points located on the nodal points in the Neumann and Dirichlet boundaries, respectively. Now the following least squares functional of all residuals at all collocation points can be constructed as:

$$J = \frac{1}{2}\left(\sum_{k=1}^{M}[R_k^{(d)}]^2 + \alpha \cdot \sum_{k=1}^{n_t}[R_k^{(t)}]^2 + \beta \cdot \sum_{k=1}^{n_u}[R_k^{(u)}]^2\right). \tag{8}$$

The parameters α and β in this equation represent the relative weight of the boundary residuals with respect to the interior residuals named as penalty coefficients.

Minimization of Eq. (8) with respect to the nodal parameters u_i leads to the following system of equations:

$$\mathbf{KU} = \mathbf{F} \tag{9}$$

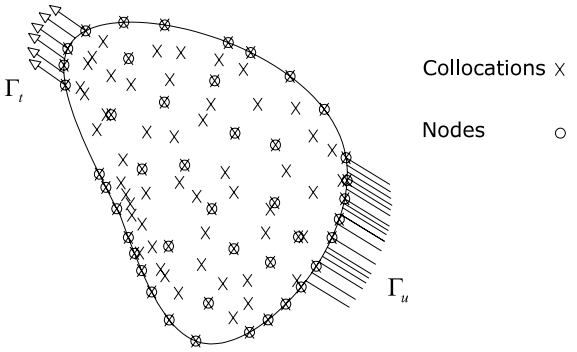

Figure 1: The domain discretized by nodal points and collocation points [5].

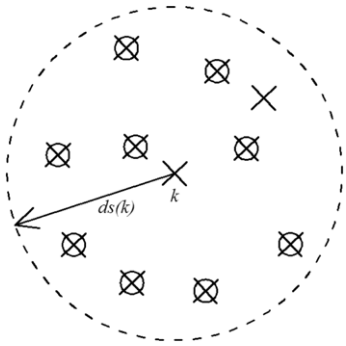

Figure 2: Compact support of kth collocation.

in which **U** is the vector of nodal parameters. The typical components of the matrix **K** and the right hand side vector **F** are defined as:

$$\begin{aligned} K_{ij} &= \sum_{k=1}^{M} L(N_i(x_k)) \cdot L(N_j(x_k)) \\ &\quad + \alpha \sum_{k=1}^{n_t} B(N_i(x_k)) \cdot B(N_j(x_k)) \\ &\quad + \beta \sum_{k=1}^{n_u} N_i(x_k).N_j(x_k) \quad i, j = 1, \ldots, n_p \end{aligned} \tag{10}$$

$$\begin{aligned} F_i &= \sum_{k=1}^{M} L(N_i(x_k))f(x_k) + \alpha \sum_{k=1}^{n_t} B(N_i(x_k))g(x_k) \\ &\quad + \beta \sum_{k=1}^{n_u} N_i(x_k) \cdot \bar{u} \quad i = 1, \ldots, n_p. \end{aligned} \tag{11}$$

The stiffness matrix **K** in Eq. (9) is symmetric even for non-self-adjoint operators. The size of **K** just depends on the number of nodal points (n_p) and the number of collocation points does not increase the size of the final system of equations. It is also sparse since a small number of nodes contribute to the function evaluation for a collocation point. Therefore the final system of equations can be solved using iterative procedures effectively.

3. Governing equations

Governing equations are comprised of continuity, momentum and constitutive equations for two dimensional incompressible flow of a generalized Newtonian fluid. They are in a non-dimensional form and Cartesian coordinates given by

$$\frac{\partial u}{\partial t} + u\frac{\partial u}{\partial x} + v\frac{\partial u}{\partial y} = -\frac{\partial P}{\partial x} + \left(\frac{\partial \tau_{xx}}{\partial x} + \frac{\partial \tau_{xy}}{\partial y}\right) \tag{12}$$

$$\frac{\partial v}{\partial t} + u\frac{\partial v}{\partial x} + v\frac{\partial v}{\partial y} = -\frac{\partial P}{\partial y} + \left(\frac{\partial \tau_{yx}}{\partial x} + \frac{\partial \tau_{yy}}{\partial y}\right) \tag{13}$$

$$\frac{\partial u}{\partial x} + \frac{\partial v}{\partial y} = 0 \tag{14}$$

$$\tau_{xx} = 2\eta\frac{\partial u}{\partial x} \tag{15}$$

$$\tau_{xy} = \tau_{yx} = \eta\left(\frac{\partial u}{\partial y} + \frac{\partial v}{\partial x}\right) \tag{16}$$

$$\tau_{yy} = 2\eta\frac{\partial v}{\partial y}, \tag{17}$$

where u, v and P are velocity components in x direction, the velocity component in y direction and pressure respectively. η is the generalized Newtonian viscosity which depends on the local shear rate (in isothermal condition). In Newtonian fluid η is constant for the entire flow field. In this study an inelastic power-law model is used to describe fluid behaviour. However any other generalized Newtonian model could also be used such as the Carreau–Yasuda model. The dimensionless form of the power-law model is given by:

$$\eta = \frac{m \cdot (\dot{\gamma})^{\frac{(n-1)}{2}}}{\mathrm{Re}}, \tag{18}$$

where $\dot{\gamma}, m, n$ and Re are second invariant of the rate of deformation tensor, fluid consistency, power-law index and Reynolds number respectively. $\dot{\gamma}$ in the Cartesian coordinate and Reynolds number are defined by

$$\dot{\gamma} = 2\left(\frac{\partial u}{\partial x}\right)^2 + 2\left(\frac{\partial v}{\partial y}\right)^2 + \left(\frac{\partial u}{\partial y} + \frac{\partial v}{\partial x}\right)^2 \tag{19}$$

$$\mathrm{Re} = \frac{\rho_0 U_0^{2-n} l_0^n}{m_0}, \tag{20}$$

where ρ_0, U_0, l_0 and m_0 are the reference values of density, velocity, length and fluid consistency. Using constitutive equations, Eqs. (12)–(13) will be:

$$\frac{\partial u}{\partial t} + u\frac{\partial u}{\partial x} + v\frac{\partial u}{\partial y} = -\frac{\partial P}{\partial x} + \left(2\frac{\partial \eta}{\partial x}\cdot\frac{\partial u}{\partial x} + \frac{\partial \eta}{\partial y}\left(\frac{\partial u}{\partial y} + \frac{\partial v}{\partial x}\right) + \eta\left(\frac{\partial^2 u}{\partial y^2} + \frac{\partial^2 u}{\partial x^2}\right)\right) \tag{21}$$

$$\frac{\partial v}{\partial t} + u\frac{\partial v}{\partial x} + v\frac{\partial v}{\partial y} = -\frac{\partial P}{\partial y} + \left(2\frac{\partial \eta}{\partial y}\cdot\frac{\partial v}{\partial y} + \frac{\partial \eta}{\partial x}\left(\frac{\partial u}{\partial y} + \frac{\partial v}{\partial x}\right) + \eta\left(\frac{\partial^2 v}{\partial y^2} + \frac{\partial^2 v}{\partial x^2}\right)\right). \tag{22}$$

The above equations are analogous to the following vectorized equation:

$$\frac{\partial \mathbf{U}}{\partial t} + u\cdot\frac{\partial \mathbf{U}}{\partial x} + v\cdot\frac{\partial \mathbf{U}}{\partial y} = -\nabla P + \left(\mathbf{A}\frac{\partial \mathbf{U}}{\partial x} + \mathbf{B}\frac{\partial \mathbf{U}}{\partial y} + \mathbf{C}\frac{\partial^2 \mathbf{U}}{\partial x^2} + \mathbf{D}\frac{\partial^2 \mathbf{U}}{\partial y^2}\right) + E. \tag{23}$$

Where:

$$\mathbf{U} = \begin{bmatrix} u \\ v \end{bmatrix}, \qquad \mathbf{A} = \begin{bmatrix} 2\dfrac{\partial \eta}{\partial x} & 0 \\ 0 & \dfrac{\partial \eta}{\partial x} \end{bmatrix},$$

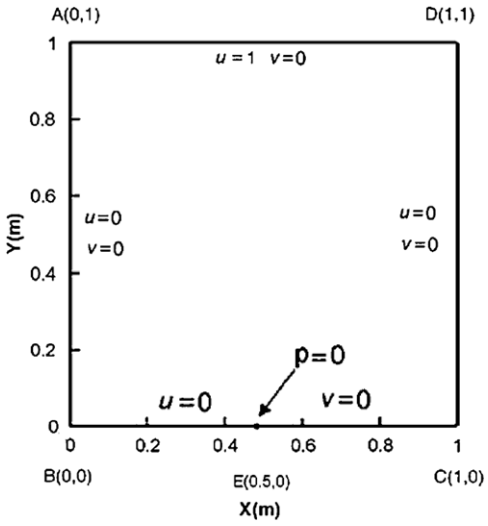

Figure 3: Boundary condition in lid-driven cavity flow problem [6].

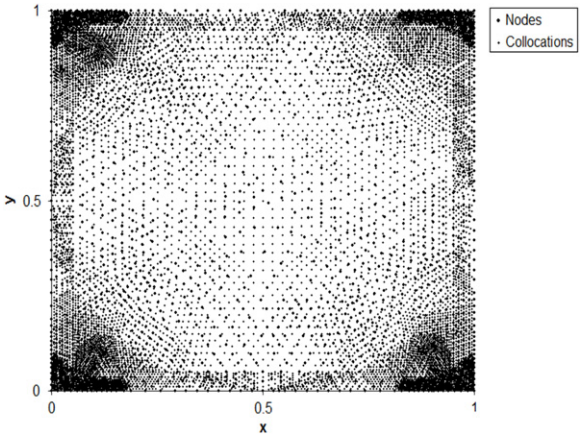

Figure 4: Points distribution in lid-driven cavity flow problem.

$$\mathbf{B} = \begin{bmatrix} \dfrac{\partial \eta}{\partial y} & 0 \\ 0 & 2\dfrac{\partial \eta}{\partial y} \end{bmatrix}, \qquad \mathbf{C} = \begin{bmatrix} \eta & 0 \\ 0 & \eta \end{bmatrix},$$

$$\mathbf{D} = \begin{bmatrix} \eta & 0 \\ 0 & \eta \end{bmatrix}, \qquad E = \begin{bmatrix} \dfrac{\partial \eta}{\partial y}\cdot\dfrac{\partial v}{\partial x} \\ \dfrac{\partial \eta}{\partial x}\cdot\dfrac{\partial u}{\partial y} \end{bmatrix}.$$

4. Temporal discretization

Temporal discretization of the momentum equations in their primitive form is carried out by the fractional step method. Several fractional step methods have been introduced in the literature. The non-incremental fractional step method proposed by Chorin [7] is one of the popular methods. In this method, a momentum equation is used to obtain the intermediate velocities by neglecting the pressure terms. It performs the advancement in time in three main steps; first, the momentum equation is used to obtain the intermediate velocity, in the next step, the pressure is evaluated using the intermediate velocity. Finally, velocity is calculated using the intermediate velocity and the pressure. The non-incremental

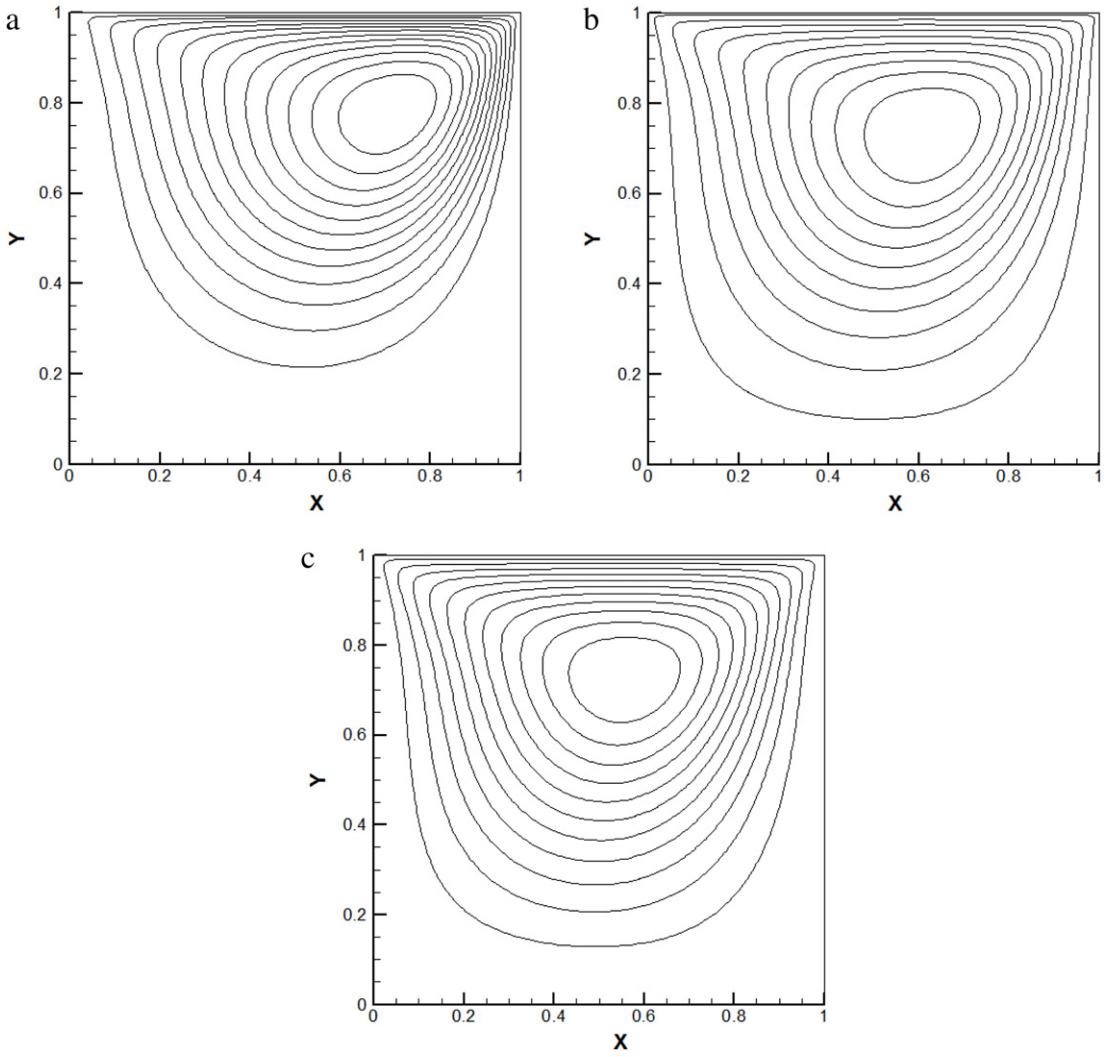

Figure 5: Stream function counters for power-law indices $n = 0.5$ (a), $n = 1$ (b), $n = 1.5$ (c).

fractional step method does not require the satisfaction of the LBB condition. This property makes this method suitable for steady state problems [8]. In this paper the non-incremental fractional step method is used in temporal discretization. As described before, first momentum equations are solved without considering the pressure terms via an implicit Euler method. It leads to the following equations:

$$\frac{\mathbf{U}^* - \mathbf{U}^\lambda}{\Delta t} + u^\lambda \cdot \frac{\partial \mathbf{U}^*}{\partial x} + v^\lambda \cdot \frac{\partial \mathbf{U}^*}{\partial y} = \left(\mathbf{A}^\lambda \frac{\partial \mathbf{U}^*}{\partial x} + \mathbf{B}^\lambda \frac{\partial \mathbf{U}^*}{\partial y} + \mathbf{C}^\lambda \frac{\partial^2 \mathbf{U}^*}{\partial x^2} + \mathbf{D}^\lambda \frac{\partial^2 \mathbf{U}^*}{\partial y^2}\right) + E^\lambda \quad (24)$$

in which $\mathbf{U}^*$ and $\mathbf{U}^\lambda$ are velocities at the intermediate and previous time step respectively. u^λ and v^λ are intermediate velocities at the previous time step. To calculate the coefficient matrix and right hand side vector, the operators L and f in Eqs. (10) and (11) for Eq. (24) can be written as:

$$L(\cdot) = (\cdot) + \Delta t \cdot u^\lambda \cdot \frac{\partial(\cdot)}{\partial x} + \Delta t \cdot v^\lambda \cdot \frac{\partial(\cdot)}{\partial y} - \Delta t \left(\mathbf{A}^\lambda \frac{\partial(\cdot)}{\partial x} + \mathbf{B}^\lambda \frac{\partial(\cdot)}{\partial y} + \mathbf{C}^\lambda \frac{\partial^2(\cdot)}{\partial x^2} + \mathbf{D}^\lambda \frac{\partial^2(\cdot)}{\partial y^2}\right) \quad (25)$$

$$f = \mathbf{U}^\lambda + \Delta t \cdot E^\lambda. \quad (26)$$

After calculating intermediate velocities (U^*), the pressure field can be obtained using the Poisson's equation for pressure.

$$\frac{\partial^2 P^{\lambda+1}}{\partial x^2} + \frac{\partial^2 P^{\lambda+1}}{\partial y^2} = \frac{1}{\Delta t}\left(\frac{\partial u^*}{\partial x} + \frac{\partial v^*}{\partial y}\right). \quad (27)$$

For Eq. (27), operators L and f can be written as below:

$$L(\cdot) = \frac{\partial^2(\cdot)}{\partial x^2} + \frac{\partial^2(\cdot)}{\partial y^2} \quad (28)$$

$$f = \frac{1}{\Delta t}\left(\frac{\partial u^*}{\partial x} + \frac{\partial v^*}{\partial y}\right). \quad (29)$$

Using these pressure values, the velocity field can be updated as follow:

$$u^{\lambda+1} = u^* - \Delta t \left(\frac{\partial P^{\lambda+1}}{\partial x}\right) \quad (30)$$

$$v^{\lambda+1} = v^* - \Delta t \left(\frac{\partial P^{\lambda+1}}{\partial y}\right). \quad (31)$$

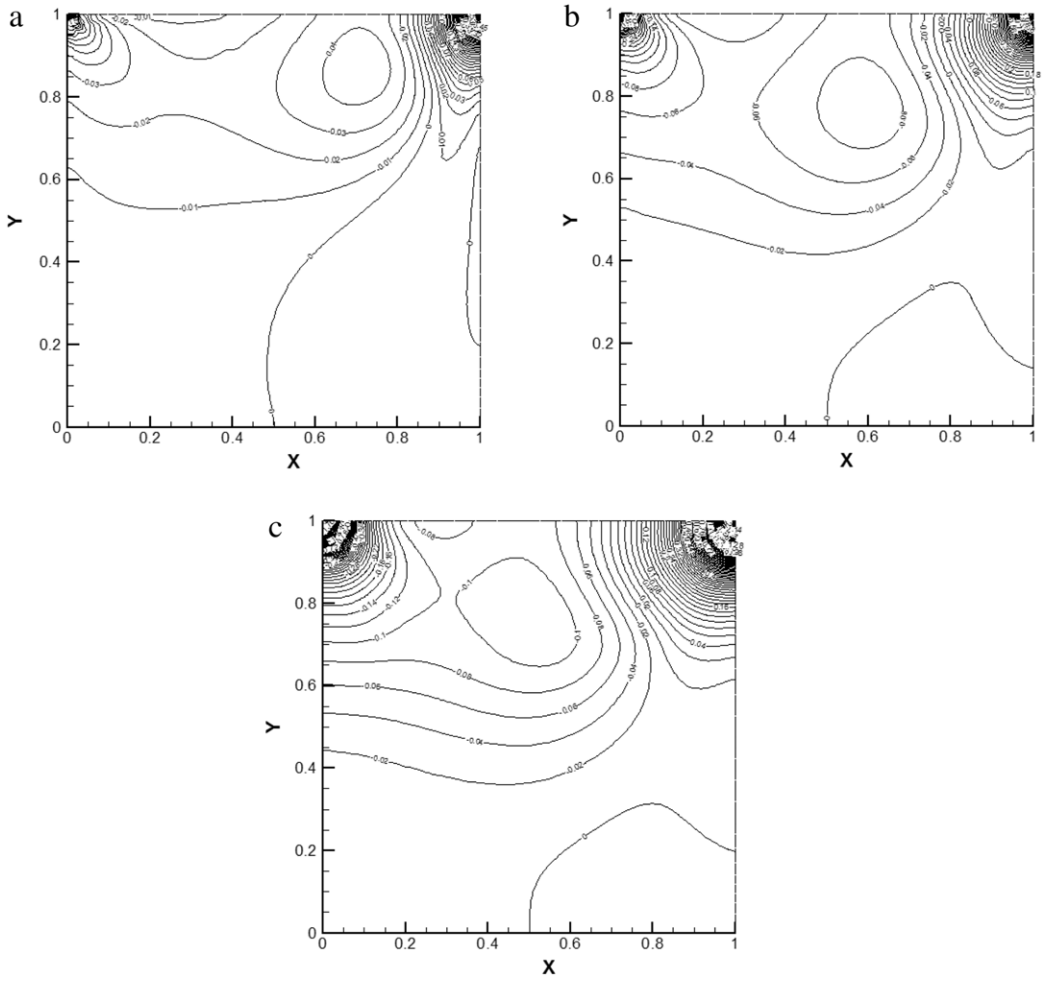

Figure 6: Pressure counters for power-law indices $n = 0.5$ (a), $n = 1$ (b), $n = 1.5$ (c).

Table 1: Wake length of flow past circular cylinder for power-law index (n) equal to 1.4 at different Reynolds numbers.

Re	Present study	Rao et al. [11]
50	0.42	0.41
100	1.01	1.05
120	1.25	1.28
140	1.51	1.48

5. Shape function construction

In this study RPIM is used to construct shape functions. Detailed descriptions of the procedure are available elsewhere [2,3]. In following numerical examples a multi quadratic radial basis function augmented with polynomials of a completed second order is used in the radial point interpolation method. The multi quadratic radial basis function (q) used in this paper, is given by:

$$q_i(r) = (ds^2 + r^2)^{2.03}, \tag{32}$$

where ds is the radius of the compact support domain defined earlier and r is the distance from the ith node. In the following numerical examples ds is always chosen for each collocation point so that 20 nodes are placed into the support domain of that collocation.

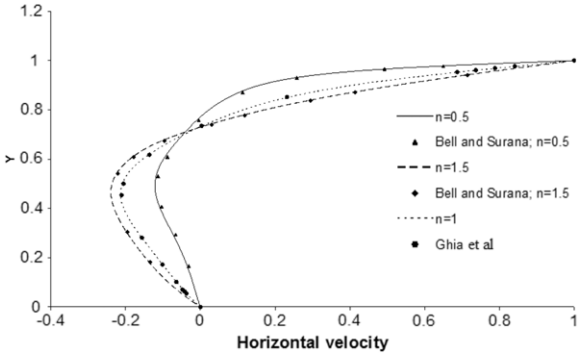

Figure 7: u profile along vertical centre line.

6. Numerical examples

The ability of the scheme is shown by solving two bench mark problems named lid-driven cavity flow and flow past a circular cylinder. In temporal discretization dealing with steady-state problems, it is favourable to use large time steps, to reduce computational cost. But large time steps may lead to an inaccurate solution because of the first order accurate time discretization that is used here. Also large time steps increase numerical diffusion which may smear the results. In the following examples the time step size is chosen to be 0.01.

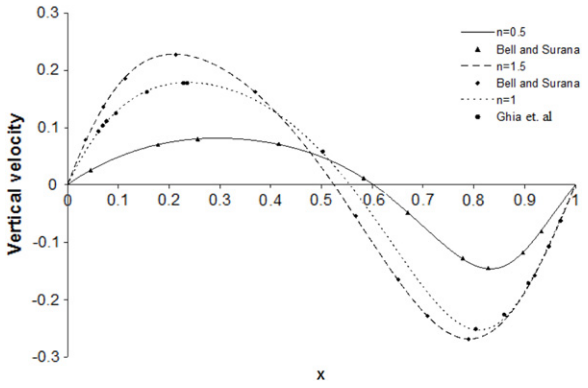

Figure 8: v profile along horizontal centre line.

Regarding penalty coefficients, they should be large enough to ensure boundary condition satisfaction. In this study, penalty coefficients are chosen to be $\alpha = \beta = 10^7$ for both problems.

6.1. Lid-driven cavity flow

One of the most popular benchmark problems in incompressible steady-state flow simulation is the lid-driven cavity flow problem. The problem is characterized by a square cavity in which the driven force for the flow is the shear created by the moving lid. The geometry and boundary conditions of this problem are shown in Figure 3. In this example Re and m are kept constantly at 100 and 1. Then the problem is solved with three values of power-law indices (n) of 0.5,1 and 1.5. In spatial discretization 2587 nodes and 11 203 collocation points are used. Point distribution is shown in Figure 4. The obtained stream functions and pressure contours are shown in Figures 5 and 6. The horizontal and vertical velocity component profiles at the mid-span of the cavity are plotted to make a comparison with Bell and Surana results [9] for the case of $n = 0.5$ and $n = 1.5$. For the case of $n = 1$, comparison is made by Ghia et al. [10] due to the fact that their work is known as one of the most detailed investigations into the cavity flow problem. The results are shown in Figures 7 and 8.

6.2. Power law fluid past a circular cylinder

As the second numerical example, the two-dimensional flow of an incompressible power law fluid past a circular cylinder placed symmetrically between two parallel plane walls is considered. Geometry and velocity boundary conditions are shown in Figure 9. Regarding pressure boundary conditions on all boundaries the derivative of pressure in the direction normal to the boundaries is considered zero except for the mid-point of the exit boundary where the value of the pressure is specified as zero. In this example power-law index (n) and fluid consistency (m) are kept constantly 1.4 and 1. The problem is solved for four different Reynolds numbers of 50,100,120 and 140. The Reynolds number calculation is based on the characteristic length of cylinder diameter ($D = 1.0$) and the characteristic velocity of free-stream velocity ($u = 1.0$). For shear-thickening fluids ($n > 1$), the flow is steady up to Re $=$ 140 for the given geometry [11]. So thanks to symmetry half the problem is solved. On the boundary of symmetry the derivative of the x-component of the velocity (u) in the direction normal to this boundary is considered zero and the y-component of the velocity (v) is set to zero. In spatial discretization 7619 nodes and 33 081 collocation points are used. Point distribution is shown in Figure 10. Obtained results of computed streamlines are plotted under a close view in Figures 11 and 12. The wake length for different Reynolds numbers, presented in Table 1, is well comparable with the results of the reference publication [11].

7. Computational costs

Since CDLS uses a local support domain in function approximation, the produced matrices are sparse. Besides that, the final coefficient matrices are symmetric. To show the computational costs of the method, the main steps along with their consumed times in solving problems 6-1 and 6-2 are given in Table 2. Consumed times are obtained on one CPU with 3.2 GHz frequency. The system of equations is solved using the DGBRTF routine in the LAPACK package [12].

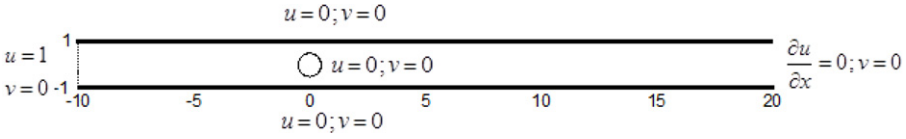

Figure 9: Geometry and velocity boundary conditions in flow past a circular cylinder problem.

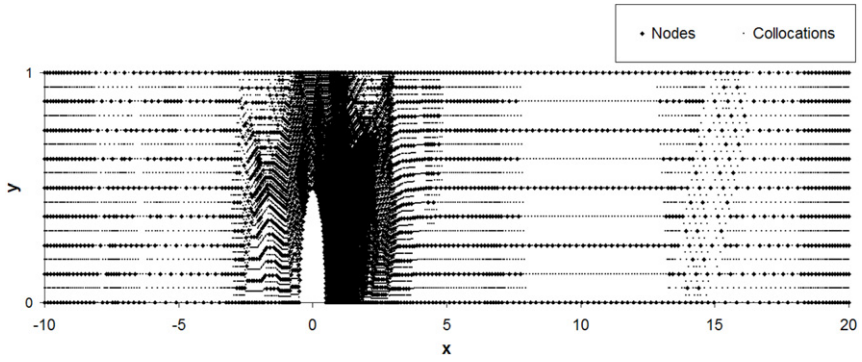

Figure 10: Points distribution in flow past a circular cylinder.

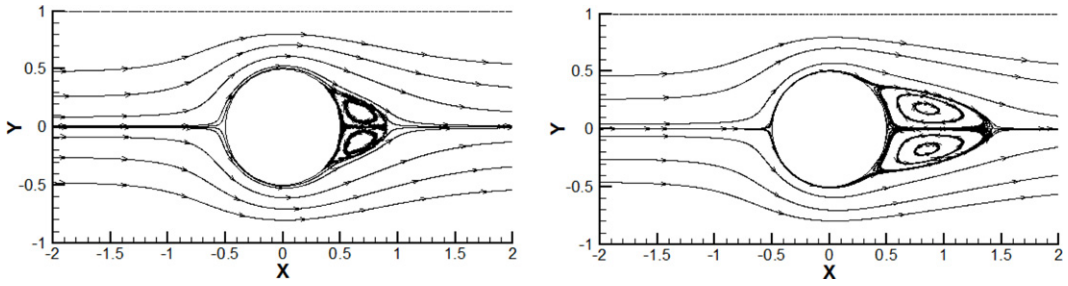

Figure 11: Stream lines at Re = 50 (left) and Re = 100 (right) for $n = 1.4$.

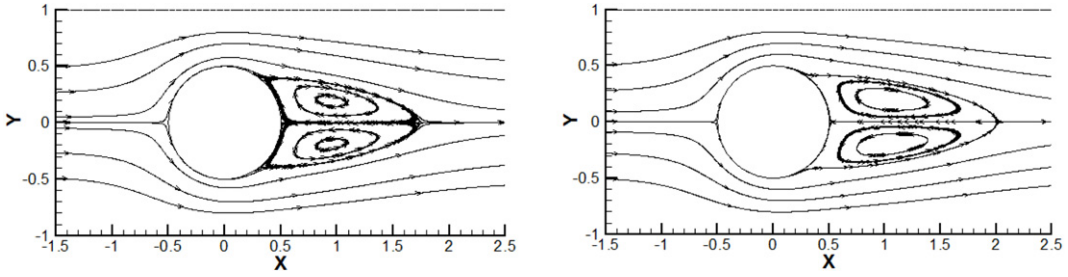

Figure 12: Stream lines at Re = 120 (left) and Re = 140 (right) for $n = 1.4$.

Table 2: Solution steps and consuming times (seconds).

Step number	Description	Consumed time for problem 6-1.	Consumed time for problem 6-2.	Remarks
1	Produce shape functions and their derivatives	10.1	21.7	This step need to be calculated just one time.
2	Solve the system of equations for u	0.06	0.27	
3	Solve the system of equations for v	0.06	0.27	These steps must be taken in every iteration
4	Solve the system of equations for p	0.06	0.27	

8. Conclusions

In the present study CDLS was extended for the solution of incompressible generalized Newtonian fluid equations. The presented formulation can be used for any generalized Newtonian model. However, in this paper it has been used for simulation of the laminar flow of power-law fluids. Two numerical examples are solved for different values of power-law indices. The computed solutions showed acceptable agreement with the solutions reported in the literature.

References

[1] Belytschko, T. "Meshless methods: an overview and recent developments", *Computer Methods in Applied Mechanics and Engineering*, 139(1–4), pp. 3–47 (1996).
[2] Liu, G.R., *Mesh Free Methods: Moving Beyond the Finite Element Method, Vol. 1*, 1st Edn., CRC Press, Boca Raton (2002).
[3] Liu, G.R. and Gu, Y.T., *An Introduction to Meshless Methods and Their Programming*, 1st Edn., Springer, Berlin (2005).
[4] Arzani, H. and Afshar, M.H. "Solving Poisson's equations by the discrete least squares meshless method", In *Boundary Elements and Other Mesh Reduction Methods XXVIII*, pp. 23–32, WIT Press, Skiathos, Greece (2006).
[5] Afshar, M.H. and Lashckarbolok, M. "Collocated discrete least-squares (CDLS) meshless method: error estimate and adaptive refinement", *International Journal for Numerical Methods in Fluids*, 56(6), pp. 1909–1928 (2008).
[6] Firoozjaee, A.R. and Afshar, M.H. "Steady-state solution of incompressible Navier–Stokes equations using discrete least-squares meshless method", *International Journal for Numerical Methods in Fluids*, 67(3), pp. 369–382 (2010).
[7] Chorin, A.J. "A numerical method for solving incompressible viscous flow problems", *Journal of Computational Physics*, 2(1), pp. 12–26 (1967).
[8] Guermond, J.L., Minev, P. and Shen, J. "An overview of projection methods for incompressible flows", *Computer Methods in Applied Mechanics and Engineering*, 195(44–47), pp. 6011–6045 (2006).
[9] Bell, B.C. and Surana, K.S. "*p*-version least squares finite element formulation for two dimensional, incompressible, non-Newtonian, isothermal and non-isothermal flow", *International Journal of Numerical Methods in Fluids*, 18, pp. 127–162 (1994).
[10] Ghia, U., Ghia, K.N and Shin, C.T. "High-Re solutions for incompressible flow using the Navier–Stokes equations and a multigrid method", *Journal of Computational Physics*, 48, pp. 387–411 (1982).
[11] Rao, M.K., Akhilesh, K. and Chhabra, R.P. "Effect of confinement on power-law fluid flow past a circular cylinder", *Polymer Engineering and Science*, Published online in Wiley Online Library (2011).
[12] Anderson, E., Bai, Z., Bischof, C., Blackford, S., Demmel, J., Dongarra, J., Du Croz, J., Greenbaum, A., Hammarling, S., McKenney, A. and Sorensen, D., *LAPACK Users' Guide*, 3rd Edn., Society for Industrial and Applied Mathematics, Philadelphia (1999).

Mohsen Lashckarbolok, received his M.Sc. degree in hydraulic structures from Iran University of Science and Technology (IUST). Now he is a Ph.D. student in IUST working on meshfree methods applications on non-Newtonian fluid flows.

Ebrahim Jabbari is Associate Professor of Civil Engineering School of the Iran University of Science & Technology. He received his Ph.D. in Hydraulic Engineering from the University of Leuven, Belgium. He has worked on numerical modeling of circulations in estuaries. Recently, he is engaged in research on numerical modeling of flow and sediment transport in rivers and coastal waters and numerical analysis of non-Newtonian fluid flow.